Electrocatalysis at graphite and carbon nanotube modified electrodes: edge-plane sites and tube ends are the reactive sites

Craig E. Banks, Trevor J. Davies, Gregory G. Wildgoose and Richard G. Compton*

Received (in Cambridge, UK) 27th August 2004, Accepted 29th September 2004
First published as an Advance Article on the web 6th December 2004
DOI: 10.1039/b413177k

Carbon, and particularly graphite in its various forms, is an attractive electrode material. Two areas of particular interest are modified carbon electrodes and carbon nanotube electrodes. In this article we focus on the relationship between surface structure and electrochemical and chemical reactivity of electrodes based on these materials. We overview recent work in this area which has led us to believe that much of the catalytic activity, electron transfer and chemical reactivity of graphitic carbon electrodes is at surface defect sites, and in particular edge-plane-like defect sites. We also question the claimed special ''catalytic'' properties of carbon nanotube modified electrodes.

1 Introduction

The effect of electrode surface structure on electroanalytical performance is widely recognised but often overlooked. For example, quite frequently electrodes that are known to possess catalytic sites (in the form of surface defects for example) are modelled as homogeneous surfaces. In this review we focus on the relationship between surface structure and the observed electrochemical (and chemical) reactivity for graphite and graphite derivatised electrodes. We report on our recent advances in this area and show how, using established electrochemical techniques, simulations and microscopy, it is possible to identify the surface sites responsible for a voltammetric response and/or chemical reaction at different carbon electrodes.

Up until the mid 1980s, all the available materials made exclusively of sp^2 hybridized carbon possessed the planar graphite sheet as their structural building block: a hexagonal lattice of 3 coordinate carbon atoms where the C–C bond length is around 1.42 Å.[1] This includes a large variety of graphite products which have been used as working electrodes, such as amorphous carbon, glassy carbon, carbon black, carbon fibres, powdered graphite, pyrolytic graphite (PG) and highly ordered pyrolytic graphite (HOPG), each with different chemical and physical properties.[1] The key structural factor that leads to such an assortment of different materials is the average graphite microcrystallite size (or lateral grain size), L_a, which is effectively the average size of the hexagonal lattices that make up the macro structure. In principle, this can range from being infinitely large, as in the case of a macro single crystal of graphite, to the size of a benzene molecule, approximately 3 Å. In practice, the smallest L_a values are found in amorphous carbon, glassy carbon and carbon black and can be as low as 10 Å.[1] Carbon fibres and pyrolytic graphite are intermediate in the range, with L_a values around 100 Å and 1000 Å respectively.[1] The largest graphite monocrystals are found in ZYA and SPI 1 grade HOPG (the highest available commercial grades of HOPG) which can be 1–10 μm in size.[1–3] Regions where individual graphite monocrystals meet each other (*i.e.* grain boundaries) are poorly defined and when exposed result in surface defects. In the case of pyrolytic graphite, the individual graphite crystallites lie along the same axis making it possible to obtain carbon surfaces with significantly less defects. This is especially true for HOPG where the large lateral grain size can result in a well defined surface with values of defect coverage as low as 0.2%.[4]

In 1985 a whole new field of sp^2 hybridised carbon structures was born with the discovery of C_{60} buckminsterfullerene.[5] Unlike the materials discussed above, C_{60} cannot be described

*Richard.Compton@chemistry.ox.ac.uk

Craig E. Banks recently completed his DPhil in the group of Professor R. G. Compton and is currently a postdoctoral research associate at the University of Oxford. His research interests are diverse encompassing all aspects of electroanalysis and sonoelectroanalysis.

Trevor J. Davies was born in Bolton, England, in 1980. He completed his MChem at the University of Oxford in 2002, where he carried out his undergraduate research in the Compton group. He has continued in the Compton group as a DPhil student. His research interests include modified carbon electrodes, HOPG electrochemistry, liquid–liquid reactions and the modelling of electrochemical systems.

Gregory G. Wildgoose was born in Derbyshire, England, in 1980. He completed his MChem at the University of Oxford in 2003, where he carried out his undergraduate research in the Compton group. He has pursued further research in the Compton group as a DPhil student. His research interests include modified carbon electrodes and derivatised carbon nanotubes, with particular emphasis on the fundamental aspects of derivatised carbon electrodes and their practical applications, in particular to the field of pH sensing.

Richard Compton is Professor of Chemistry in the Physical and Theoretical Chemistry Laboratory at the University of Oxford and a Fellow and Tutor in Chemistry at St. John's College. He has broad research interests in electrochemistry, interfacial kinetics and electroanalysis.

by planar graphite sheets, but rather possesses the truncated icosahedral structure—a polygon with 60 vertices and 32 faces, 12 of which are pentagonal and 20 hexagonal.[5] Although a large amount of electrochemical experiments were performed with C_{60} and other "bucky balls",[6] carbon structures of this type were never considered as possible electrode materials due to their poor conductivity. This all changed in 1991 with Iijima's discovery of carbon nanotubes which, amongst other noticeable properties, possessed excellent electrical conductivity.[7] The basic carbon nanotube structure can be thought of as a seamless "rolled up" rectangular sheet of graphite resulting in a single tube of 2–30 nm in diameter and several microns in length (multiwalled carbon nanotubes, where several tubes are found one inside the other, are discussed later).[8] Indeed, the open ends of carbon nanotubes have been likened to the edge-planes of HOPG with the tube walls suggested to have properties similar to those of the basal plane of HOPG.[9] Electrochemical experiments utilising carbon nanotubes as the working electrode have shown what appears to be enhanced electron transfer reactivity compared to other electrode materials for a variety of systems.[10] This is especially true in the case of biological molecules such as NADH,[11] dopamine,[12] cytochrome c,[13] azurin,[14] horseradish peroxidase,[15] and DNA,[16] where carbon nanotubes are becoming increasingly attractive for electroanalytical applications.[10]

The following work is divided into three sections. First, we discuss our progress in simulating the voltammetry of electrode surfaces that contain defects and apply it to the case of basal plane HOPG. The results suggest that surface defects in the form of exposed edge-plane nanobands play a major role in the voltammetry of basal plane HOPG. Second, we explore the relevance of this edge-plane activity to working electrodes composed of modified carbon nanotubes, with special attention to the site of chemical and physical adsorption. Finally, we look at cases where carbon nanotubes have possibly been mislabelled as "electro-catalytic" and show how their electrochemical response is often similar to that of edge-plane graphite.

2 Exploring the relationship between electrode surface structure and the observed electron transfer reactivity

2.1 Electrochemically heterogeneous electrodes

Within the layered structure of graphite we can identify two types of graphitic plane: the basal plane, containing all the atoms of a particular graphite layer, and the edge-plane, perpendicular to the basal plane. Due to the nature of the chemical bonding in graphite, the two planes display noticeably different electrochemical properties. For example, for most redox couples the electrode kinetics at edge-plane graphite are considerably faster than at basal plane graphite.[17] Therefore, a carbon electrode surface consisting of edge and basal plane graphite will be an electrochemically heterogeneous electrode (EHE), where the redox reaction is described by two sets of electrode kinetics:

edge-plane:

$$A + e^- \xrightleftharpoons{k^\circ_{edge}, \alpha_{edge}} B$$

(A)

basal plane:

$$A + e^- \xrightleftharpoons{k^\circ_{edge}, \alpha_{edge}} B$$

in which k°_i and α_i are the standard electron transfer rate constant and symmetry coefficient for electrode material i (i = edge or basal). In the following section we discuss our progress in understanding the electrochemical properties of these two types of graphite by simulating the cyclic voltammetry of simple one electron redox couples (described by pathway A) at basal plane HOPG, a well defined carbon surface.

2.2 The diffusion domain approach

The basal plane surface of an HOPG electrode consists of layers of graphite which lie parallel to the surface and are separated from each other by 3.35 Å.[18] Surface defects occur in the form of steps exposing the edges of the graphite layers as illustrated in Fig. 1. The distance between these defects can be no greater than the lateral grain size of the graphite sample, which in the case of HOPG is 1–10 μm (for the grade of HOPG used in this work).[3] Thus, as the steps are multiples of 3.35 Å deep and typically range between 1–20 layers for HOPG, the total surface coverage of edge-plane graphite is rather small.

For example, McCreery and co-workers have shown *via* STM that the total coverage of edge-plane defects can be as low as 0.2% (cleavage with adhesive tape results in significantly more surface defects).[4] Although it is widely accepted that these edge-plane defects have a major influence on the voltammetry of basal plane HOPG, when trying to fit experimental data to theoretical simulations most research workers treat the HOPG surface as homogeneous, and assume linear diffusion to the whole of the electrode surface.

Indeed, when simulating the cyclic voltammetry of basal plane HOPG electrodes, not only do we need to take into account this inherent heterogeneity, due to the size of the spacing between edge-plane defects, non-linear diffusion will be significant and a 2-dimensional simulation is necessary.[19] The influence of non-linear diffusion on the cyclic voltammetric response of an electrode is shown by the schematic in Fig. 2(a), which essentially illustrates the transition between macro and microelectrode behaviour. As we decrease the size of the electrode (with respect to the diffusion layer thickness) the contribution of convergent diffusion to the voltammetry increases such that we achieve faster mast transport per unit area of the electrode resulting in larger current densities and voltammograms which appear increasingly distorted from the well documented macro electrode shape.[20]

Fig. 2(b) illustrates the situation for an array of microelectrodes. In this case the second electrode material is inert but the same principles apply. At the start of the scan, the individual electrodes are independent, each with their own undisturbed diffusion layer, Fig. 2(b)(i), and the voltammetric response displays the characteristics of the individual microelectrodes. What happens as the scan progresses depends on the size of the diffusion layer thickness *vs.* the size of the spacing between the electrodes. At some point the diffusion layers of adjacent microelectrodes may start to overlap

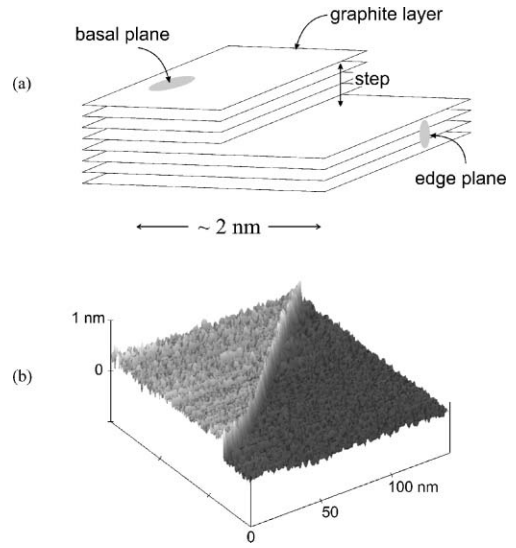

Fig. 1 (a) Schematic diagram of a 4 layer step edge. (b) Scanning tunnelling microscopy image of a mono layer step on a HOPG surface (grade SPI 1 equivalent to ZYA).

resulting in a situation where solution on the "overlapping region" is depleted by more than one electrode. Accordingly, the voltammetric response will no longer resemble that of individual microelectrodes but rather display characteristics similar to macroelectrode cyclic voltammetry, where solution depletion results in a well defined peak, as opposed to the steady state like limiting plateau observed for microelectrodes.

The extreme of this diffusion layer overlap is complete diffusion over the whole surface, such that the concentration at a height z above the inert material is equal to that at a point z metres above a microelectrode. As illustrated in Fig. 2(b)(iii), this results in linear concentration profiles and therefore, voltammetry attributable to planar diffusion. Whether this extreme is ever reached and the time elapsed before the diffusion layers overlap depends on a number of parameters, such as the scan rate, the diffusion coefficient and the size of the surface inhomogeneities. At 1.0 V s^{-1} with a diffusion coefficient of 1×10^{-5} cm^2 s^{-1} (typical cyclic voltammetry and aqueous solution parameters), on reaching the first peak potential in a cyclic scan the diffusion layer generated should be no greater than $\sim$15 μm. On a basal plane HOPG surface, the distance between steps can be up to 1–10 μm. Hence, a HOPG voltammogram will be affected by overlapping diffusion layers and a 2-dimensional simulation is necessary.

Using today's numerical methods, a 2-dimensional simulation of the whole electrode surface would not be possible. Rather, we need to introduce approximations and break the problem down into smaller, more manageable pieces. One way of achieving this is *via* the diffusion domain approach, first introduced by Amatore *et al.* for the simulation of regular microelectrode arrays.[21] We can approximate each basal plane island and the surrounding edge-plane band as a circular disc of edge-plane graphite partially (or almost completely) covered with basal plane graphite, such that the areas of edge and basal plane are consistent, as shown in Fig. 3(a). Because our island and band are surrounded by other island/band combinations, little or zero net flux of electroactive species will pass from one

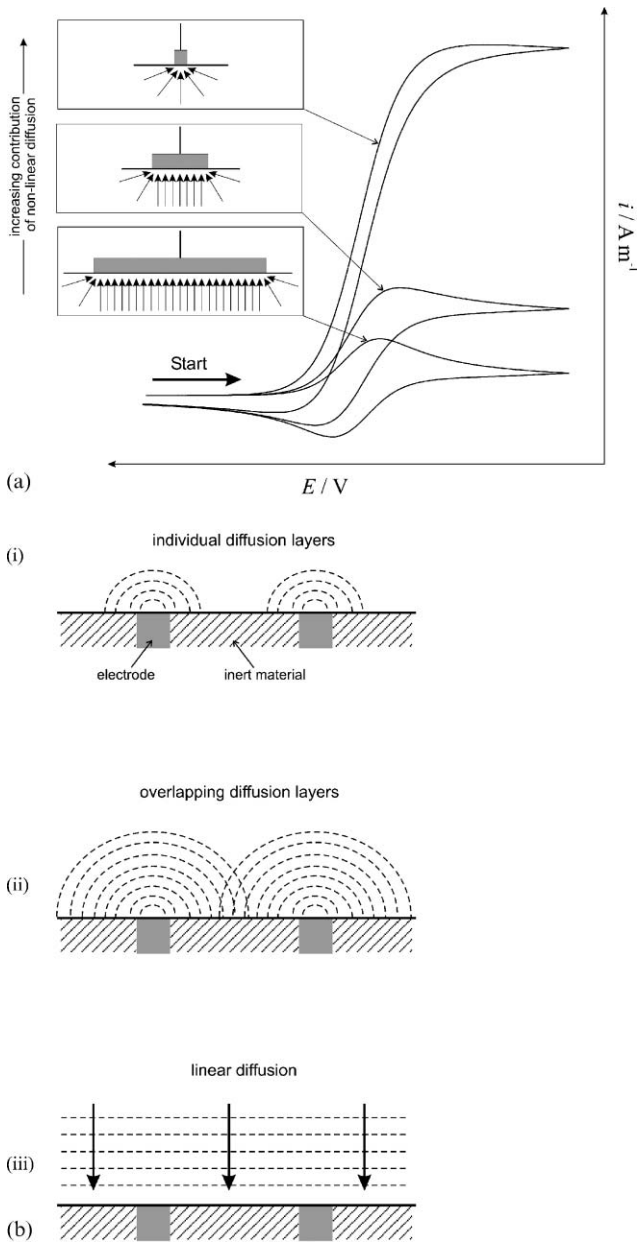

Fig. 2 (a) Schematic diagram showing the relationship between the size of the electrode (with respect to the diffusion layer thickness) and the contribution of convergent diffusion to the observed voltammetry. (b) Illustration of the interaction of neighbouring diffusion layers.

island to its neighbour. Thus, we can consider these circular discs as independent entities with cylindrical walls through which no net flux can pass. These unit cells are better known as diffusion domains and an example is illustrated in Fig. 3(b) where we have also assigned the two electrode materials. The whole electrode surface can be considered as an ensemble of these diffusion domains of varying size and coverage. Therefore, to simulate the cyclic voltammetry of our EHE we simply sum the cyclic voltammograms of every diffusion domain on the electrode surface.[19] It should be noted that this diffusion domain approach can be and has been applied to a wide range of systems, including the study of liquid–liquid reactions at microdroplet modified electrodes.[22,23]

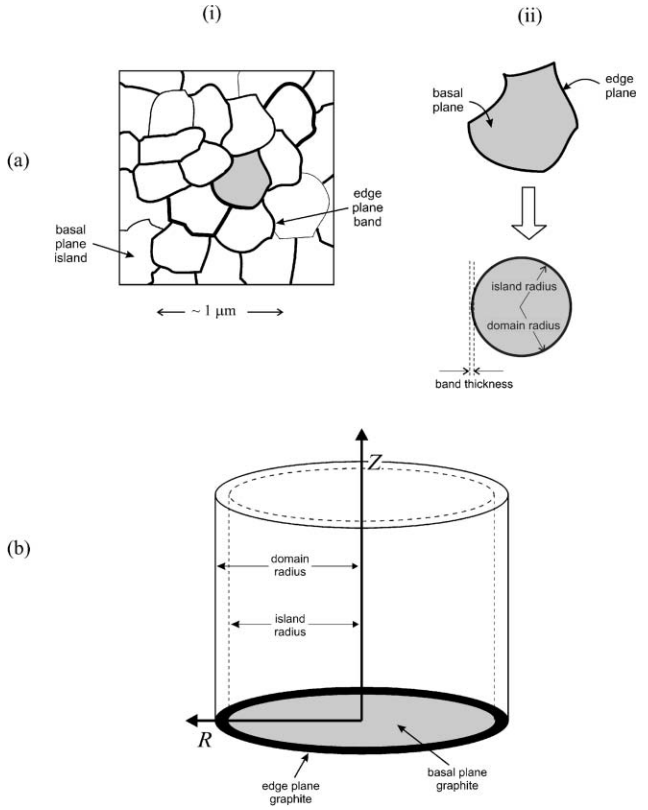

Fig. 3 (a) Schematic diagrams showing (i) the overhead view of a section of the basal plane HOPG surface and (ii) the approximation of each island/band combination as a partially covered circular disc of the same area. (b) The resulting diffusion domain from the approximation in (a)(ii) and the cylindrical coordinate system employed.

2.3 Explaining the characteristics of HOPG voltammograms

Fig. 4 illustrates a cyclic voltammogram for the oxidation of 1.0 mM ferrocyanide in 1.0 M KCl solution at (i) a basal plane HOPG electrode and (ii) an edge-plane pyrolytic graphite (eppg) electrode where the scan rate is 1.0 V s^{-1}. Overlaid as a dashed curve is the simulated "linear diffusion only" voltammogram (obtained *via* DigiSim©[24]) that best fits the HOPG voltammogram. The figure clearly illustrates the two major characteristics of HOPG voltammograms. First, we observe a significant increase in peak to peak separation over its eppg counterpart suggesting much slower electrode kinetics. Second, the fit to a "linear diffusion only" simulation is poor, especially in the second half of the scan where we observe a significantly lower peak current than expected.[17,25] McCreery and co-workers have shown that a better fit between theory and experiment is obtained by, rather arbitrarily, incorporating a potential dependent α into the simulations,[25] but this still treats the HOPG surface as homogeneous, despite the guaranteed presence of surface defects. If we are to explain these characteristics we need first to consider the voltammetry of individual domains and then expand our argument to the ensemble.

Assuming $\alpha = 0.5$ (and $d\alpha/dE = 0$) for both materials, we can obtain $k\mathrm{E}_{\mathrm{edge}}$ from comparison of the eppg voltammogram with DigiSim© leaving us with the problem of assigning a value for $k\mathrm{E}_{\mathrm{basal}}$. In Fig. 4 the best fit linear diffusion only voltammogram corresponds to an electron transfer rate constant of 6.2×10^{-6} cm s^{-1}. As discussed above, this value is an effective electron transfer rate constant, $k\mathrm{E}_{\mathrm{eff}}$, and should not be assigned to the basal plane because the surface contains edge-plane defects. Indeed, it is well documented that the peak to peak separation observed for HOPG voltammograms depends on the surface defect density: the lower the amount of edge-plane defects, the higher the observed ΔE_{p} and hence the lower the value of k°_{eff}. HOPG surfaces with the lowest defect densities have yielded k°_{eff} values for the oxidation of ferrocyanide of the order 10^{-9} cm s^{-1}.[26] For the time being, let us assume that this value of $k^{\circ}_{\mathrm{eff}} = 10^{-9}$ cm s^{-1} corresponds to a basal plane HOPG surface with no defects such that $k^{\circ}_{\mathrm{basal}} = 10^{-9}$ cm s^{-1}. Fig. 5 illustrates simulated voltammograms for diffusion domains of increasing size where $k\mathrm{E}_{\mathrm{edge}} = 0.022$ cm s^{-1} (from the DigiSim© fit to Fig. 4(ii)), $k\mathrm{E}_{\mathrm{basal}} = 10^{-9}$ cm s^{-1}, the edge-plane band thickness corresponds to a 6 layer step and the rest of the parameters are given in the figure legend. Overlaid in each plot is the voltammogram for the case where $k\mathrm{E}_{\mathrm{basal}} = 0$ cm s^{-1} (*i.e.* the basal plane is inert), the rest of the parameters being the same. In each of the plots the current has been normalised according to eqn. 1

$$\psi = \frac{I}{[\mathrm{A}]_{\mathrm{bulk}} A_{\mathrm{elec}} \sqrt{\frac{F^3 D v}{RT}}} \qquad (1)$$

in which I is the current, $[\mathrm{A}]_{\mathrm{bulk}}$ is the initial concentration of species A, A_{elec} is the electrode (or domain) area, F is the Faraday constant, D is the diffusion coefficient of species A, v is the scan rate, R is the molar gas constant and T is the temperature. This allows an easy comparison to cyclic voltammetry at macroelectrodes for which the peak dimensionless current varies between 0.3506 (irreversible) and 0.4463 (reversible) for a one electron redox reaction where $\alpha = 0.5$ at 298 K.[27]

Taking the four parts of the figure into account, three things become apparent. First, the peak to peak separation of the edge-plane nano band signal strongly depends on the edge-plane coverage, θ_{edge} (*i.e.* the defect density). Second, the basal plane with $k\mathrm{E}_{\mathrm{basal}} = 10^{-9}$ cm s^{-1} has little or no influence on the voltammetry of the three smaller domains. This is due to the depleting effect of non-linear diffusion which becomes less relevant as the domain size increases. Therefore, since the maximum lateral grain size for the HOPG studied is 1–10 μm resulting in a maximum R_0 of ~0.5–5 μm, the edge-plane coverage is such that we can consider the basal plane as *effectively* inert, *i.e.* the HOPG response in Fig. 4 can be assigned to nano bands of edge-plane graphite with the basal plane islands having no contribution to the observed voltammogram. Third, and most importantly, can we be sure that 10^{-9} cm s^{-1} is an accurate value for $k^{\circ}_{\mathrm{basal}}$? If so, then according to Fig. 5(c), a strangely distorted voltammogram would be expected in the limit of very low defect density. Despite all the work on the oxidation of ferrocyanide at HOPG electrodes carried out in the past,[17,25,26,28,29] such a signal has never been reported. As seen in Figs. 5(a)–(d), the smaller the coverage of edge-plane, the larger the peak to peak separation. Thus, it seems more plausible that the rate of electron transfer for the oxidation of ferrocyanide at basal

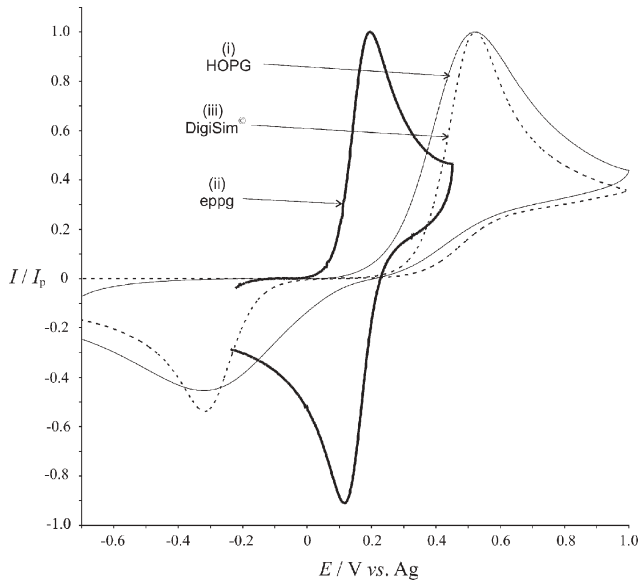

Fig. 4 Cyclic voltammograms recorded at 1 V s^{-1} for the oxidation of 1 mM ferrocyanide in 1 M KCl solution at (i) a basal plane HOPG electrode and (ii) an edge-plane pyrolytic graphite electrode. The dashed voltammogram (iii) is the simulated DigiSim© fit to (i).

plane graphite is far lower than 10^{-9} cm s^{-1}, possibly even zero, such that we can attribute all ferrocyanide voltammetry recorded at HOPG electrodes to the edge-plane defects (whether the basal plane is actually inert or $k\mathrm{E}_{\mathrm{basal}}$ is less than 10^{-9} cm s^{-1} is currently under investigation). Indeed, the same applies to other redox couples, not just ferrocyanide.[19]

Fig. 6 illustrates how a linear diffusion cyclic voltammogram fits to the four inert voltammograms in Fig. 5. As observed, not all the voltammograms are a perfect fit to DigiSim©. As we increase R_0, the inert voltammograms become more distorted with respect to their linear fit. Both the forward and backward peaks are widened and the reverse peaks become considerably smaller in magnitude than their linear counterparts—exactly the same characteristics as observed in Fig. 4. The reason we see this change is due to a 2-dimensional diffusional effect and is discussed in detail in ref. 19. As mentioned previously, domain radii of approximately 1 μm and less are expected on our HOPG surface so some of the domains that contribute to the observed voltammetry will themselves have a distorted ψ-E curve. It transpires that when summing the voltammograms for all the domains present on the electrode surface, these distortions remain or are enhanced, thus explaining the source of voltammogram distortion.[19]

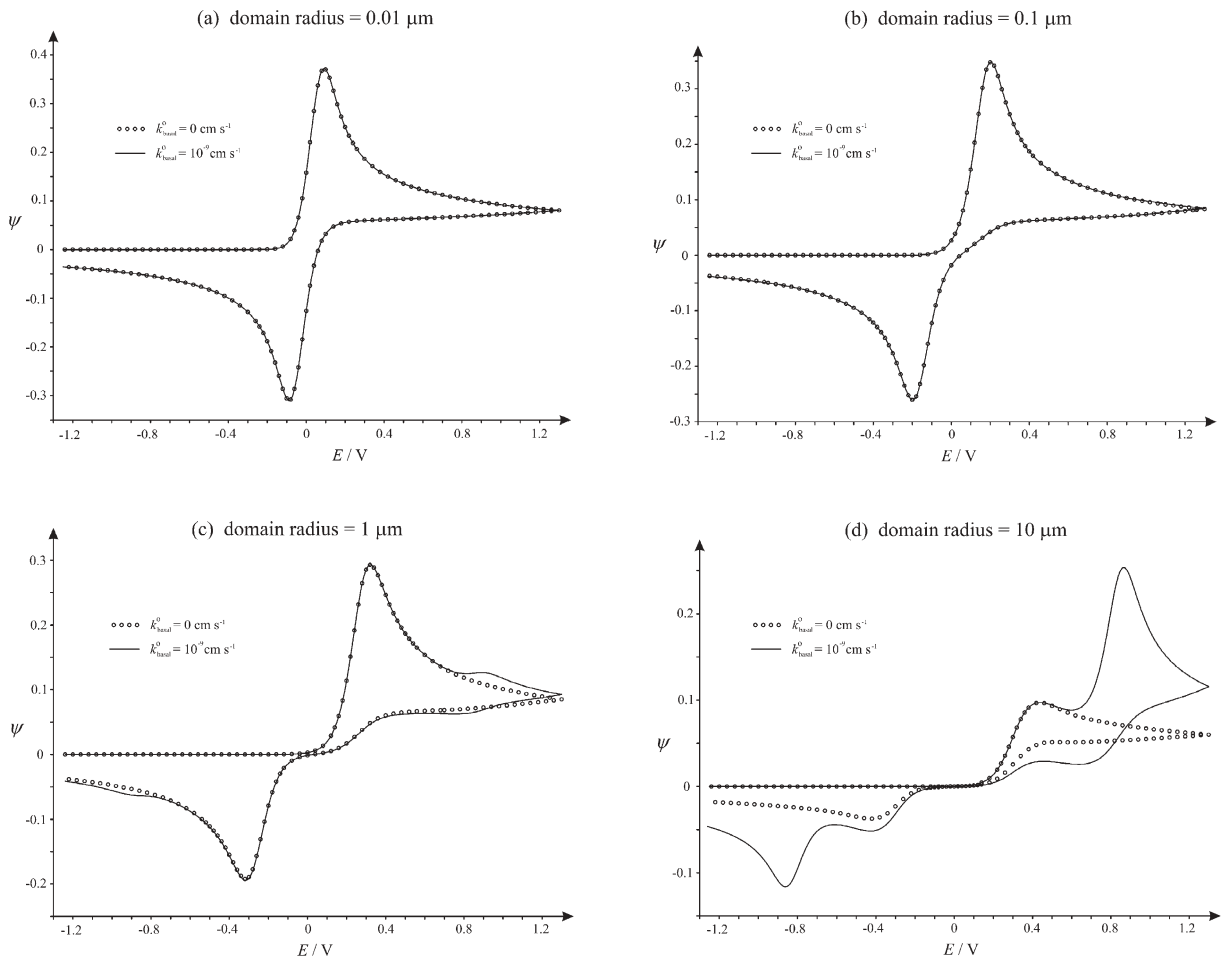

Fig. 5 The solid curves are simulated dimensionless current cyclic voltammograms for diffusion domains where $D = 6.1 \times 10^{-6}\,\mathrm{cm^2\,s^{-1}}$, $k\mathrm{E}_{\mathrm{edge}} = 0.022\,\mathrm{cm\,s^{-1}}$, $k\mathrm{E}_{\mathrm{basal}} = 10^{-9}\,\mathrm{cm\,s^{-1}}$, $v = 1\,\mathrm{V\,s^{-1}}$, the band thickness is 1.005 nm and the domain radius is (a) 0.01 μm, (b) 0.1 μm, (c) 1 μm and (d) 10 μm. Overlaid in each section are the simulated inert equivalents (o), *i.e.* $k\mathrm{E}_{\mathrm{basal}} = 0\,\mathrm{cm\,s^{-1}}$. In all diffusion domain simulations $\alpha = 0.5$ and $\mathrm{d}\alpha/\mathrm{d}E = 0$.

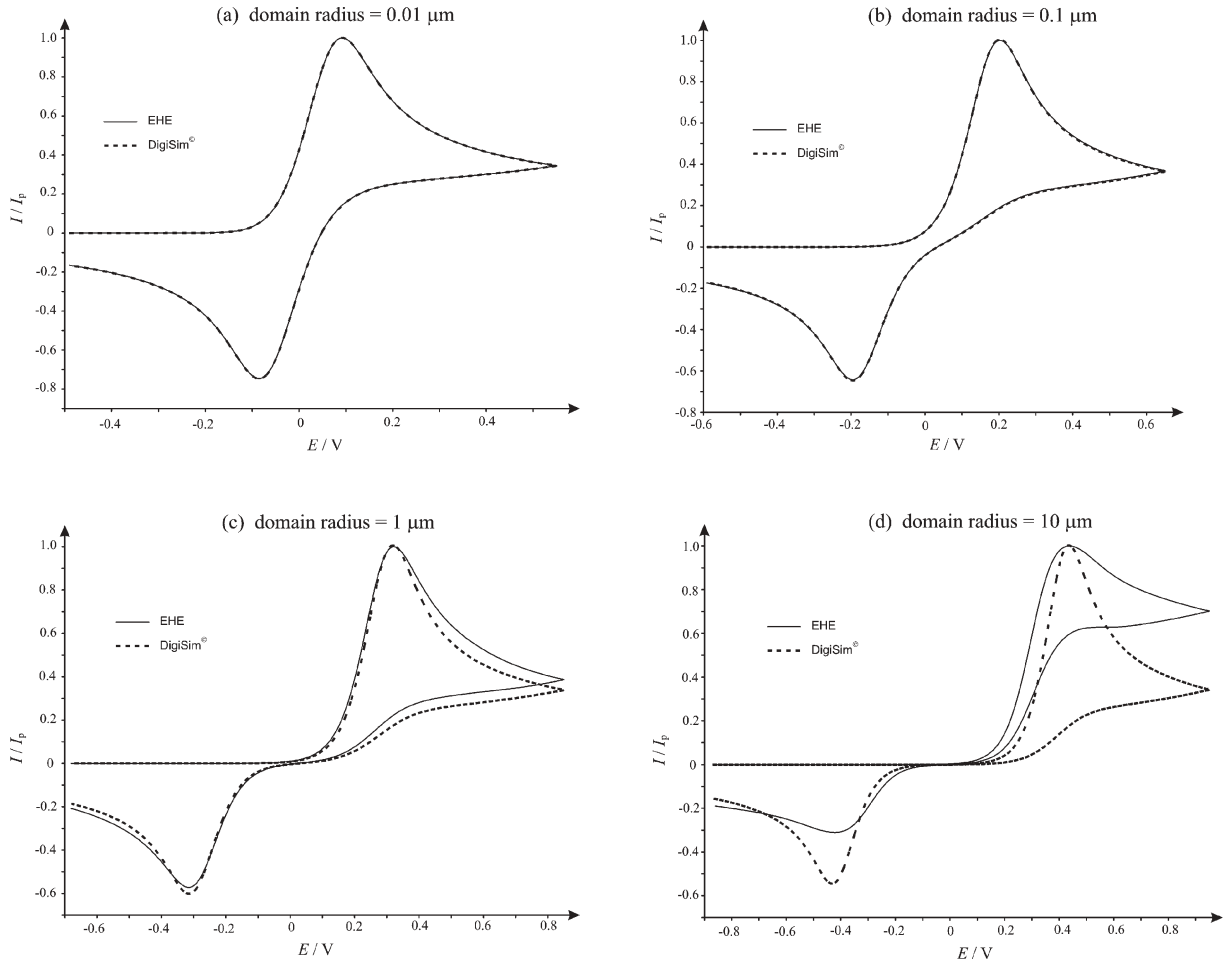

Fig. 6 Comparison of the inert voltammograms in Fig. 5 with their best fits to a simulated linear diffusion voltammogram.

Due to the fact that there are so many unknowns in our problem, our diffusion domain approach can only supply data of a qualitative standard with regard to the HOPG surface. However, using further approximations, we have developed a protocol to estimate the fractional coverage of edge-plane defects on the HOPG surface *via* a very simple cyclic voltammetry technique.[19] A more quantitative application of this 2-dimensional Butler–Volmer simulation has been illustrated in the determination of the coverage of gold particles on modified edge-plane carbon.[19]

In summary, basal plane HOPG can be considered a ''special'' carbon material in that it has a very small coverage of edge-plane defects separated by relatively large distances. It is these two properties that lead to distorted voltammograms with large peak to peak separations. By taking the inherent surface heterogeneity into account, we have shown *via* our simulations that the voltammetry of basal plane HOPG is consistent with that for an array of edge-plane nano bands with the basal plane being effectively inert (whether $k\mathrm{E}_{\mathrm{basal}}$ is zero or extremely small is currently under investigation). Furthermore, as shown in Figs. 6(a) and (b), if the spacing between defects is too small, the overall CV response should be a good fit to DigiSim©. In other words, we *cannot* associate a perfect fit to DigiSim© with linear diffusion to a homogeneous surface. It transpires that only HOPG has a lateral grain size large enough to observe the ''tell-tale'' signs of edge-plane activity and basal plane inertness. Therefore, even though other carbon materials might not show the same voltammetric characteristics as HOPG, there is no reason why the conclusions from our HOPG studies cannot be applied to different carbon materials such as the more disordered basal plane pyrolytic graphite or glassy carbon, for example. This also includes carbon nanotubes, the walls of which should be similar to basal plane graphite with the tube ends comparable to edge-plane graphite.

3 Modification of multiwalled carbon nanotubes leading to activity primarily at edge-plane defects

Over the past decade there has been an increasing interest in tailoring electrode surfaces to impart desired properties for catalysis, analysis or biological applications (see refs. 30–34 and references contained therein). Carbon electrodes have proved particularly easy to modify. This can be achieved either through physical adsorption of the modifier onto the carbon surface, or by covalently attaching the modifier. Covalent bond formation is activated either electrochemically such as the direct electro-oxidation of amines[34,35] or the reduction of aryl diazonium salts[34,36] or chemically such as the reduction of aryl diazonium salts by treatment with hypophosphorous

acid.[30,33,37–39] In recent years much of this research has focused on modifying carbon nanotubes (CNTs) in various ways.

Since their discovery in 1991 by Iijima[7] a wide variety of CNTs and carbon nanoparticles have been produced. The two principle forms of CNTs are single walled (SWCNT) and multiwalled carbon nanotubes (MWCNT). Structurally, SWCNTs consist of a single tube of ''rolled up'' graphite sheet where as MWCNTs consist of several concentric tubes of graphite fitted one inside the other. The diameter of a CNT can range from just a few nanometers in the case of SWCNTs to tens of nanometers for MWCNTs. There is some morphological variation possible in MWCNTs which is dependant on the conditions and the chosen method of CNT formation *e.g.* chemical vapour deposition or the high voltage arc method.[40] They can be produced in ''hollow-tube'' form where the axis of the graphite planes is parallel to the axis of the nanotube, ''herringbone'' form[40] where the graphite planes are formed at an angle to the axis of the tube or finally in a ''bamboo-like'' form[41] which is similar to the herringbone form except that the nanotubes are periodically closed along the length of the tube into compartments rather like bamboo or a ''stack of paper cups fitted one inside the other'' (Scheme 1). In the latter two cases, as the axis of the graphite planes are at an angle to the nanotube itself, a high proportion of the graphite sheets must terminate at the surface of the tube giving rise to a large number of edge-plane or edge-plane-like defect sites along the surface of the tube. As discussed in sections 2.3 and 4.1, we believe that it is these edge-plane-like defects that are responsible for much of the electrochemical activity of the CNTs compared to the smooth, more basal-plane like regions along the CNT surface.

However, the heterogeneous nature of graphitic electrode surfaces, including CNTs, affects not only the electron transfer properties of the graphitic material, but it also has an important influence on the modification of the carbon surface by redox active organic molecules. This has been illustrated by recent work carried out in this laboratory on the derivatisation of ''bamboo-like'' multiwalled carbon nanotubes (MWCNTs, 30 ± 10 nm diameter, 5–20 μm length) which possess a large number of edge-plane-like surface sites. These studies have led us to conclude that edge-plane or edge-plane-like defects on the surface of the MWCNTs may be the active sites for the chemically activated covalent attachment of aryl moieties such as 1-anthraquinonyl and 4-nitrophenyl groups as well as the partial intercalation of 4-nitrobenzylamine (4-NBA).

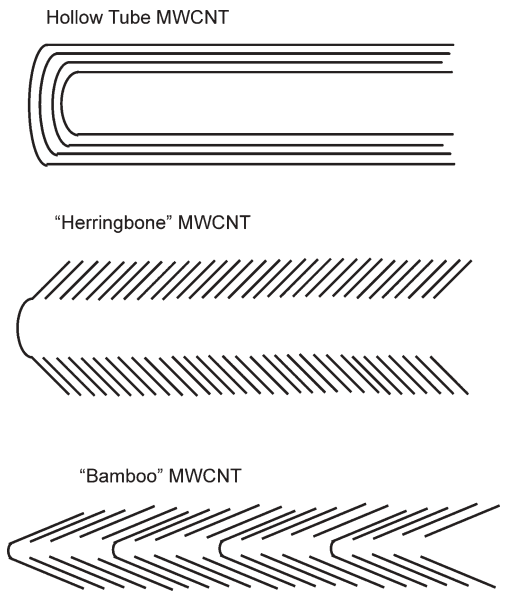

Scheme 1 A schematic cross-section through a ''hollow-tube'', ''herringbone'' and ''bamboo'' MWCNT showing the orientation of the graphene sheets within the tube.

3.1 Partial intercalation of 4-nitrobenzylamine into edge-plane-like surface defects on multiwalled carbon nanotubes

We have attempted to modify multiwalled carbon nanotubes (MWCNTs) in a variety of ways such as the formation of agglomerates of MWCNTs[31] and the chemical reduction of aryl diazonium salts onto the surface of the MWCNTs.[33]

Whilst attempting to covalently attach 4-nitrobenzylamine (4-NBA) to the surface of MWCNTs *via* the chemical oxidation of the benzylic amine group to the corresponding radical cation, we observed that simply stirring 50 mg of MWCNTs in degassed acetonitrile containing 10 mM 4-NBA for two hours led to surface modification without the presence of an oxidising agent.

Characterisation of the modified MWCNTs using cyclic voltammetry and an established protocol described in more detail in ref. 32 revealed that the 4-NBA had indeed modified the surface of the MWCNTs. The 4-NBA modified MWCNTs (4-NBA–MWCNTs) produced a stable voltammetric response, characteristic of the reduction of the nitro group moiety in aqueous solutions containing 0.1 M KCl as a supporting electrolyte from pH 1.0 to pH 12.0 (Fig. 7) and in non-aqueous solutions of acetonitrile containing either 0.1 M tetrabutyl-ammonium perchlorate (TBAP) or 0.1 M $LiClO_4$ as a supporting electrolyte (Figs. 8 and 9 respectively).[32] In order to determine exactly how the 4-NBA had modified the MWCNTs, we carried out further experiments.

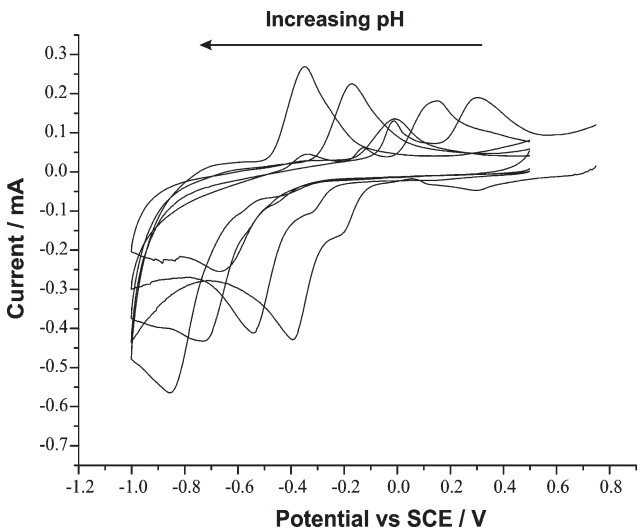

Fig. 7 The first cyclic voltammograms (overlaid) of 4-NBA–MWCNTs recorded in solutions of varying pH (pH 1.0, 4.6, 6.8, 9.2 and 12.0).

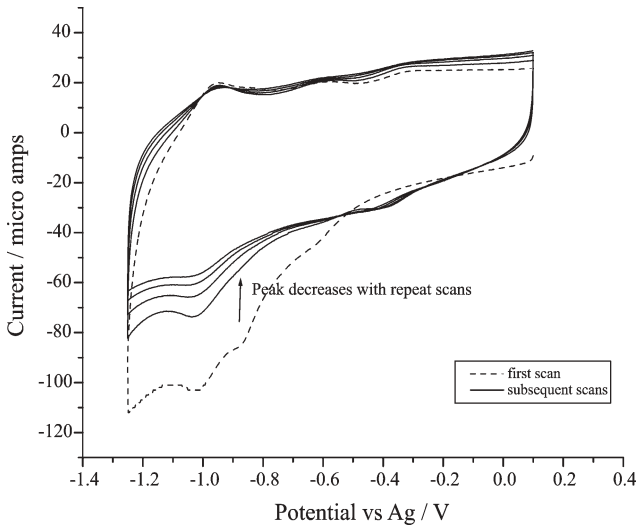

Fig. 8 Five consecutive cyclic voltammograms of 4-NBA–MWCNTs in acetonitrile containing 0.1 M TBAP.

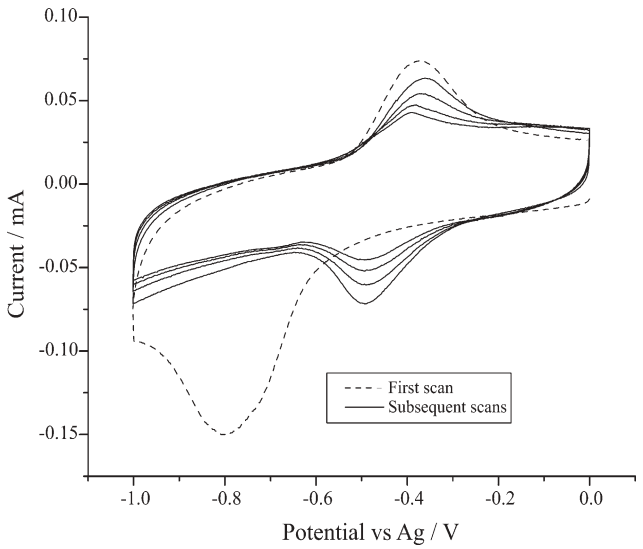

Fig. 9 Five consecutive cyclic voltammograms of 4-NBA–MWCNTs in acetonitrile containing 0.1 M $LiClO_4$.

Physical adsorption or chemisorption of 4-NBA onto the MWCNT surface were excluded as possible mechanisms for 4-NBA modification due to the reaction conditions employed providing no driving force for physisorption or chemisorption and voltammetric evidence to the contrary.[32]

Full intercalation could be ruled out as the 4-NBA molecule is simply too big to fully intercalate deep within the MWCNT layers (interlayer spacing 3.41 Å).[42]

However, during the course of our investigation we have produced evidence that tentatively supports our theory of partial intercalation of the 4-NBA. This could only take place at edge-plane or edge-plane-like defect sites on the surface of the MWCNTs. The first piece of evidence is that if we carry out cyclic voltammetry in dry acetonitrile using 0.1 M $LiClO_4$ as a supporting electrolyte (Fig. 9), very different voltammetry is observed from the case where 0.1 M TBAP is used as the electrolyte (Fig. 8). In fact the voltammetry corresponds to that of aqueous nitro reduction electrochemistry despite the acetonitrile being relatively dry. Furthermore, the 4-NBA remains stable on the MWCNTs when immersed in acetonitrile for over a week. However if the 4-NBA–MWCNTs are then electrochemically reduced in the presence of lithium, the voltammetric response appears to originate from 4-NBA in solution. To explain this result we propose that 4-NBA is partially intercalated between the graphite layers on the carbon surface as in Scheme 2. Upon initial reduction, lithium cations, which are well known to complex to nitro groups and facilitate further reduction,[43,44] complex to the 4-NBA and the material

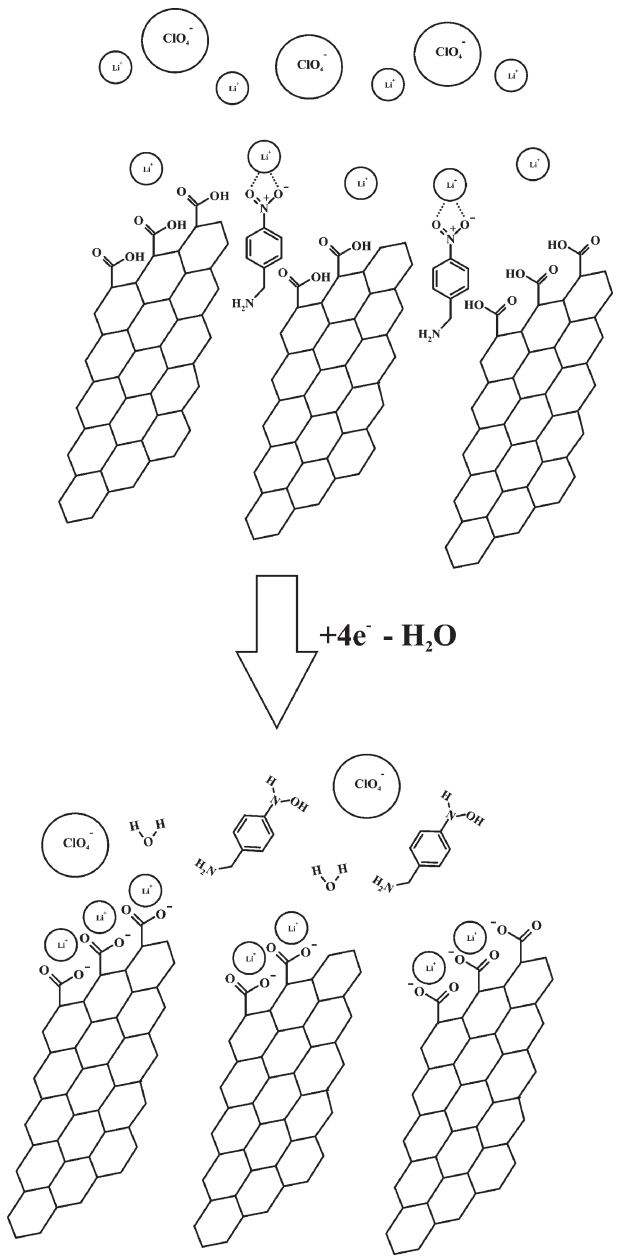

Scheme 2 A schematic diagram illustrating the proposed mechanism for the electrochemical reduction of partially intercalated 4-NBA in acetonitrile containing 0.1 M $LiClO_4$. The participation of carboxylic acid groups on the carbon surface is also represented. (No attempt has been made to accurately describe the "double layer"!)

is further reduced to the arylhydroxylamine in a manner analogous to the electrochemical reduction of 4-NBA in aqueous solution. In this case, the protons are supplied by the surface carboxylic acid groups.[43] Ion-pairing to the lithium cation induces the reduced 4-NBA molecules to desorb from the MWCNT surface and into the diffusion layer. Hence the voltammetric response rapidly dies away on subsequent cycles or if the solution is gently stirred.[32]

Further evidence for partial intercalation arises from scanning electron microscopy (SEM) images which reveal that the average diameter of the MWCNTs after derivatisation with 4-NBA has increased from an average of 40 nm to 60 nm. High resolution transmission electron microscopy (HRTEM) of the unmodified MWCNTs reveals that the MWCNTs consist of "bamboo-like" regions (Fig. 10). In these "bamboo-like" regions, the planes of the graphite sheets are at an angle to the axis of the nanotube itself. Thus every sheet must terminate at an edge-plane-like surface defect. This leads us to believe that it is these defect sites that are the active sites for partial intercalation of 4-NBA into the MWCNT. This theory is supported by X-ray powder diffraction studies.

The X-ray diffractograms of MWCNTs before and after modification with 4-NBA reveal that there has been no shift in peak position (Fig. 11). However, after modification with 4-NBA, the half-height peak-width has increased and the peak has become asymmetrical with a small tail on the left hand edge of the peak. This is characteristic of an increase in the disorder amongst the crystal layers and indeed the analysis of the half-height full-width before and after derivatisation using the Scherrer equation revealed that the average number of ordered graphite layers in the MWCNTs had decreased from nine to six. However these must be localised effects as the peak position, *i.e.* the average interlayer spacing, had remained the same. We therefore propose that 4-NBA modifies the surface of MWCNTs by partially intercalating into edge-plane and edge-plane-like defects according to Scheme 3. This leads to an increase in the average tube diameter as observed by SEM ($d_2 > d_1$ in Scheme 3). The average interlayer spacing remains the same but the disorder between the layers has increased in agreement with the X-ray powder diffraction results. Thus we conclude that the presence of edge-plane defects is crucial to this modification process.

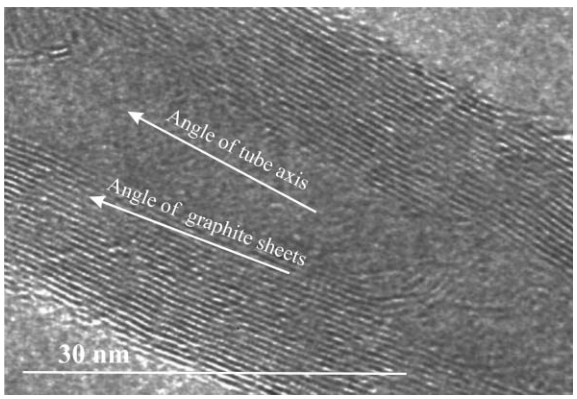

Fig. 10 High resolution transmission electron microscopy image of a "bamboo-like" region of a MWCNT.

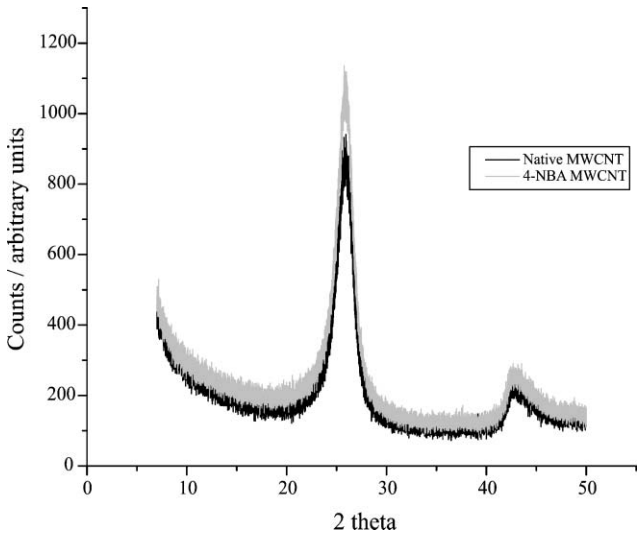

Fig. 11 X-Ray powder diffractograms comparing unmodified MWCNTs with 4-NBA modified MWCNTs.

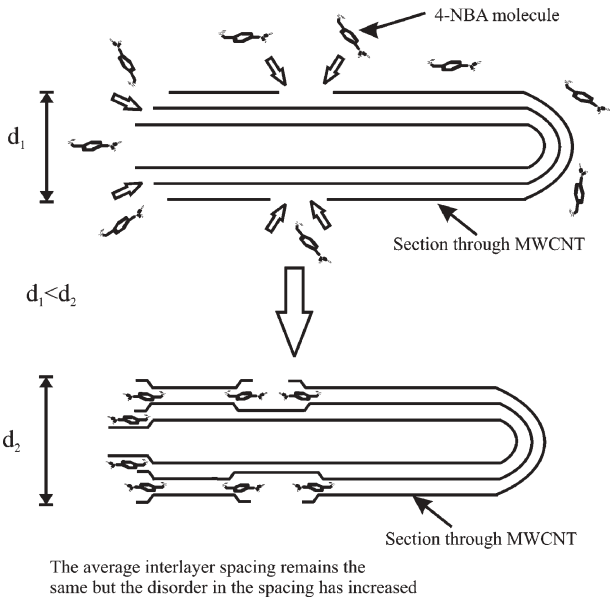

Scheme 3 A schematic diagram illustrating the proposed partial intercalation of 4-NBA into localised edge-plane defect sites along the surface of a MWCNT.

3.2 Covalent bonding of anthraquinonyl radicals to the surface of MWCNTs

Further evidence for the important role of edge-plane-like sites on the surface of MWCNTs is illustrated by the covalent modification of MWCNTs with aryl diazonium salts. This has been achieved by the direct electrochemical activation of the aryl diazonium salt,[34,36] initiating the formation of a covalent bond between the aryl group and the MWCNT. To this end, the aryl diazonium salt undergoes a one electron reduction at the electrode surface with subsequent loss of N_2 and the formation of the corresponding aryl radical which can then form a covalent bond with the electrode surface. We have developed a new method of derivatising carbon surfaces using chemical rather than electrochemical activation of the aryl

diazonium salt *via* its reduction with hypophosphorous acid.[30,33,37–39] To demonstrate the versatility of this method, we have covalently derivatised MWCNTs with 1-anthraquinonyl and 4-nitrophenyl groups from the corresponding diazonium salts (Scheme 4).[20] To achieve this we employed the following derivatisation procedure: first 50 mg of MWCNTs were stirred into 10 cm^3 of a 5 mM solution of either Fast Red AL (anthraquinone-1-diazonium chloride) or Fast Red GG (4-nitrobenzenediazonium tetrafluoroborate), to which 50 cm^3 of hypophosphorous acid (H_3PO_2, 50% w/w in water) were added. Next the solution was allowed to stand at 5 °C for 30 minutes with gentle stirring. After which, the solution was filtered by water suction in order to remove any unreacted species from the MWCNT surface. Further washing with deionised water was carried out to remove any excess acid and finally with acetonitrile to remove any unreacted diazonium salt from the mixture. The derivatised MWCNTs were then air-dried by placing them inside a fume hood for a period of 12 hours after which they were stored in an airtight container prior to use.[30,33,37–39]

The 1-anthraquinonyl or 4-nitrophenyl derivatised MWCNTs (AQ–MWCNTs and NB–MWCNTs respectively) were characterised voltammetrically and were found to be covalently attached to the surface of the MWCNTs.[33] These materials were found to respond to changes in pH over a wide pH range (pH 1.0 to 12.0) and at elevated temperatures up to 70 °C (Fig. 12).[33] Having established that we can initiate covalent bonding to the MWCNTs through chemical activation of the aryl diazonium salt, we must consider the likely site of attack by the aryl radical during derivatisation. The most likely site for covalent bond formation between the graphene

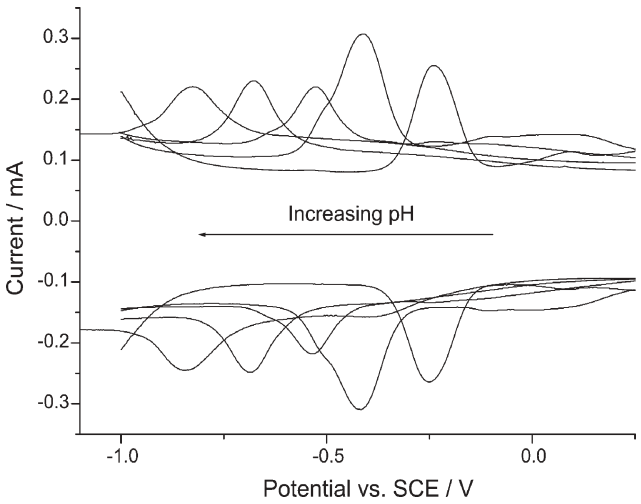

Fig. 12 Overlaid oxidative and reductive square wave voltammograms of AQ–MWCNTs at 303 K with varying pH (pH 1.0, 4.6, 6.8, 9.2 and 12.0).

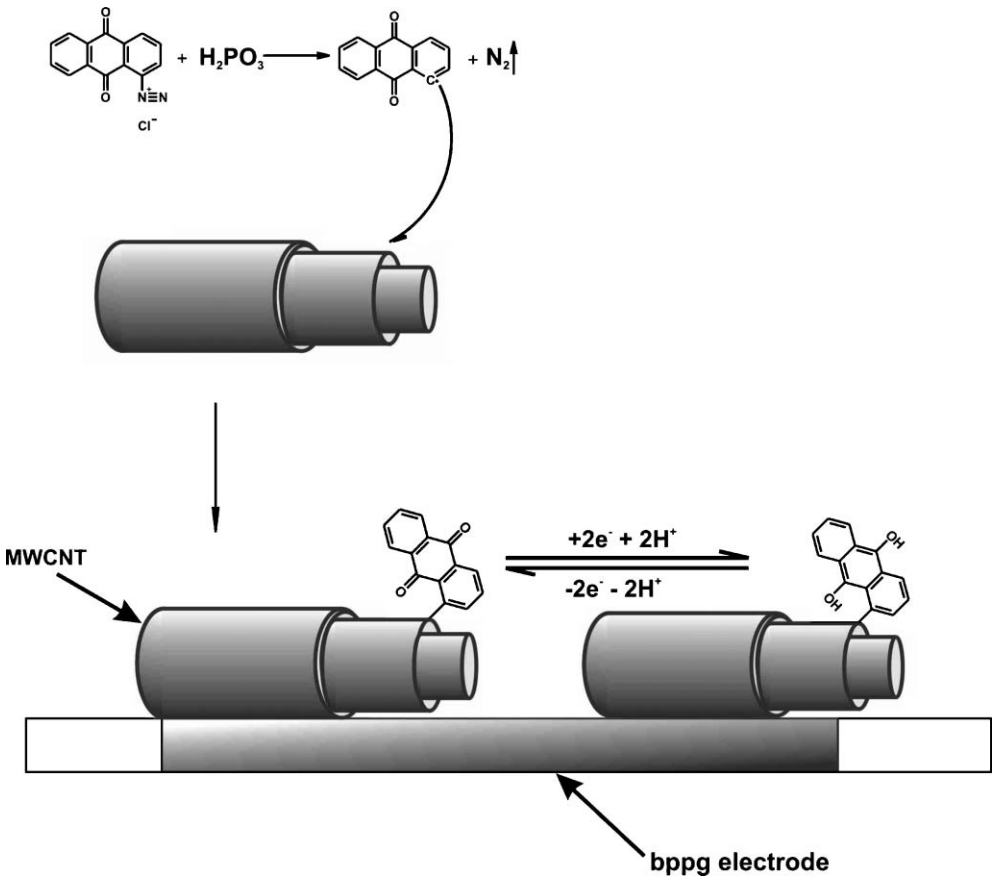

Scheme 4 A cartoon of the derivatisation by the reduction of anthraquinone-1-diazonium chloride using hypophosphorous acid, subsequent attack of the 1-anthraquinonyl radical onto the edge-plane sites on a MWCNT, and redox behaviour after abrasive immobilization onto a bppg electrode in aqueous media.

sheets of the MWCNT and the aryl radical is at edge-plane sites along the nanotube. As discussed previously in section 2.3, electron transfer and much of the surface activity of graphite-like materials has been shown to occur primarily at edge-plane sites on the surface. As covalent bond formation between the aryl radical and the MWCNT requires electron transfer from both the radical and the carbon surface it is likely that the derivatisation of MWCNTs by aryl radicals must also occur at these sites (Scheme 4). Indeed it has been reported in studies where chemisorption is initiated *via* electrochemical reduction of aryl diazonium salts that the corresponding aryl radical produced aggressively attacks the surface of carbon electrodes at both edge and basal plane sites but that attack at edge-plane sites is preferential as the kinetics of bond formation at basal plane sites appear to be significantly slower than at edge-plane defect sites.[36,45–48] A quantitative comparison between the rates of chemisorption of aryl diazonium salts to MWCNTs containing a high proportion of edge-plane-like defect sites (''bamboo-like'' and ''herringbone-like'' MWCNTs) and MWCNTs which are predominantly smooth-walled hollow tubes with a high proportion of basal plane character is part of the ongoing research being carried out in this laboratory.

We now present some of our recent work on the effects of edge-plane activity in CNTs used for analytical and catalytic purposes and seek to dispel some of the myths surrounding CNTs' claimed ''catalytic'' properties. In particular the discussion in section 2 perhaps suggests that the key structural features of CNTs for electrochemical reactions are the edge-plane-like nanotube ends rather than the nanotube body itself.

4 Electrocatalytic properties of carbon nanotubes

4.1 Identification of the electrocatalytic properties of carbon nanotubes

Our first suspicion of the properties of edge-plane-like effects were noted when we investigated the oxidations of NADH, epinephrine, and norepinephrine using abrasively modified MWCNT basal plane pyrolytic graphite (bppg) electrodes. Electrocatalytic behavior was observed for the nanotube modified electrode but when the CNTs are replaced with carbon powder, similarly enhanced currents and analogously reduced peak-to-peak separations in the voltammetry in comparison with naked basal plane pyrolytic graphite were observed.[49] This was investigated further.

First we considered the electrochemical reduction of ferricyanide (in 0.1 M KCl) using a MW-carbon nanotube film-modified basal plane pyrolytic graphite electrode. Cyclic voltammograms were recorded over a range of scan rates. Fig. 13 shows the voltammetric response, which has a peak-to-peak separation of 58 mV, suggesting fast electron transfer. The response can be compared with that from a bare basal plane pyrolytic graphite electrode and from a C_{60} film modified electrode: the voltammetric responses are shown in Fig. 13 where the C_{60} modified and naked graphite electrodes have peak-to-peak separations of 350 mV and 550 mV (at 100 mV s^{-1}) respectively, suggesting that the nanotubes are 'electrocatalytic'. In the case of the C_{60} film, the modification of the electrode surface serves to act as inert particles, resulting

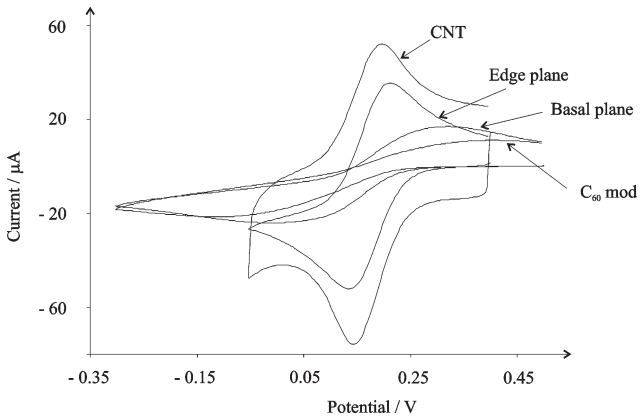

Fig. 13 Cyclic voltammograms of C_{60} abrasively and film modified bppg electrodes (4.9 mm diameter) for the reduction of 1 mM ferricyanide (in 0.1M KCl). Also shown is the response of a bare bppg electrode. All are recorded at a scan rate of 100 mV s^{-1}.

in a partially blocked electrode surface, which appears to slow down the rate of electron transfer. Next the response of an edge-plane pyrolytic graphite electrode was sought. This was found to exhibit a peak-to-peak separation of 78 mV, which is close to the response at the nanotube modified electrode. It can be inferred that the electrochemical reaction occurs with a roughly similar rate constant for both CNT film modified basal plane and bare edge-plane pyrolytic graphite electrodes. The slight difference in electron transfer rates between the edge-plane pyrolytic graphite electrode and carbon nanotube modified electrodes may reflect the presence of some basal plane defect in the edge-plane pyrolytic graphite.

To further emphasize the above observation, the electrochemical oxidation of epinephrine was studied. First the responses of a CNT modified electrode and an edge-plane pyrolytic graphite electrode were compared. As depicted in Fig. 14, the CNT film modified electrode has oxidation and reduction peaks at +0.41 ($\pm$0.01) V and −0.23 ($\pm$0.01) V, respectively (*vs.* SCE). For the edge-plane electrode the oxidation peak is observed at +0.38 ($\pm$0.01) V which is virtually identical to the oxidation potential observed at the carbon nanotube modified electrode. In comparison, the bare and C_{60} film modified bppg electrodes exhibit irreversible oxidation peaks at +0.57 ($\pm$0.01) V and +0.64 ($\pm$0.01) V respectively, suggesting slower electron transfer at these electrodes.

Comparison of the modified carbon nanotube bppg electrode with edge-plane pyrolytic graphite electrodes suggests that the electrocatalytic properties of carbon nanotubes are due to edge-plane like sites which occur at the open ends of the nanotubes.[50] Therefore, for electroanalysis on a range of redox systems, there is no significant advantage of using carbon nanotube modified electrodes over edge-plane pyrolytic graphite electrodes, as exemplified in the direct electrochemical oxidation of homocysteine, *N*-acetylcysteine, cysteine and glutathione. For each thiol, the electrocatalysis seen at nanotube modified electrodes was mirrored in the results seen at edge-plane electrodes, providing a simple, sensitive and cheap sensing protocol, and effectively replacing the need for a carbon nanotube modified electrode in electrochemical

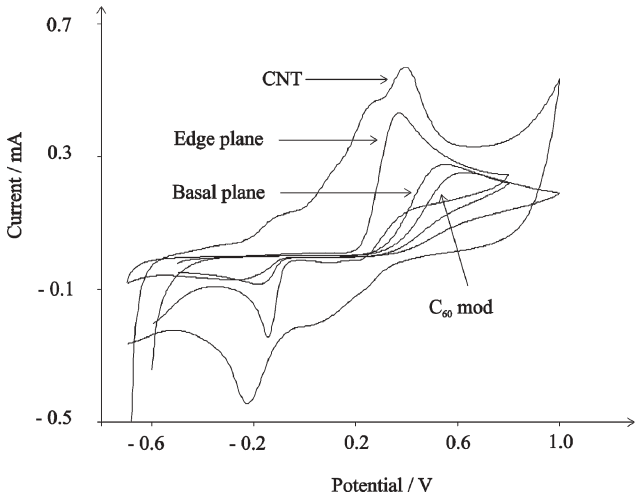

Fig. 14 Cyclic voltammograms for the oxidation of 1 mM epinephrine (in pH 5 buffer) for CNT and C_{60} film modified bppg electrodes compared with a bare bppg electrode and an edge-plane pyrolytic graphite electrode. *All at a scan rate of 100 mV* s^{-1}. Note the current for **all** the CV's except the CNT modified have been multiplied by a factor of 4 for clarity (see text for details).

contexts.[50] That said, in a number of cases the molecules under detection can interact with carbon nanotubes in a way that a well polished "traditional" carbon electrode cannot, and it is this combination of edge-plane like electro-reactivity with the special morphology and small size of CNTs that can lead to important applications. For example, in an electrochemical study of natural DNA, Wang and co-workers obtained a large signal enhancement when using CNT modified electrodes compared to glassy carbon.[16] They proposed the CNTs could cause the DNA to unwrap, thus exposing the primary redox sites right next to the site of electron transfer.[16] In addition, there remain some systems where CNTs appear to have greatly increased electro-reactivity compared to "traditional" carbon electrodes. For example, Wang *et al.* have found that Nafion coated CNTs can oxidize hydrogen peroxide at unusually low potentials.[51]

Acknowledgements

CEB and TJD thank the EPSRC for support *via* project studentships. GGW thanks the BBSRC and Schlumberger Cambridge Research for financial support. The authors thank Mr David L. Carnahan of Nano-Lab Inc. and Michael Hyde for providing the HRTEM and STM images respectively.

Craig E. Banks, Trevor J. Davies, Gregory G. Wildgoose and Richard G. Compton*
Physical and Theoretical Chemistry Laboratory, Oxford University, South Parks Road, Oxford, UK OX1 3QZ.
E-mail: Richard.Compton@chemistry.ox.ac.uk; Fax: +44 01865 275410; Tel: +44 01865 275413

References

1 R. L. McCreery, in *Electroanalytical Chemistry*, ed. A. J. Bard, Marcel Dekker, New York, 1990, vol. 17, p. 221.
2 A. W. Moore, in *Chemistry and Physics of Carbon*, ed. P. L. Walker and P. A. Thrower, Marcel Dekker, New York, 1973, vol. 11, p. 69.
3 See "http://www.2spi.com/catalog/new/hopgsub.shtml".
4 M. T. McDermott and R. L. McCreery, *Langmuir*, 1994, **10**, 4307.
5 H. W. Kroto, J. R. Heath, S. C. O'Brien, R. F. Curl and E. E. Smalley, *Nature*, 1985, **318**, 162.
6 B. S. Sherigara, W. Kutner and F. D'Souza, *Electroanalysis*, 2003, **15**, 753.
7 S. Iijima, *Nature*, 1991, **56**, 354.
8 C. N. R. Rao, B. C. Satishkumar, A. Govindaraj and M. Nath, *ChemPhysChem*, 2001, **2**, 78.
9 J. J. Gooding, R. Wibowo, J. Liu, W. Yang, D. Losic, S. Orbons, F. J. Mearns, J. G. Shapter and D. B. Hibbert, *J. Am. Chem. Soc.*, 2003, **125**, 9006.
10 E. Katz and I. Willner, *ChemPhysChem*, 2004, **5**, 1084.
11 J. Wang and M. Musameh, *Anal. Chem.*, 2003, **75**, 2075.
12 P. J. Britto, K. S. V. Santhanam and P. M. Ajayan, *Bioelectrochem. Bioenerg.*, 1996, **41**, 121.
13 G. Wang, J. J. Xu and H. Y. Chen, *Electrochem. Commun.*, 2002, **4**, 506.
14 J. J. Davis, R. J. Coles and H. A. O. Hill, *J. Electroanal. Chem.*, 1997, **440**, 279.
15 Y. D. Zhao, W. D. Zhang, H. Chen, Q. M. Luo and S. F. Y. Li, *Sens. Actuators, B*, 2002, **87**, 168.
16 J. Wang, M. Li, Z. Shi, N. Li and Z. Gu, *Electroanalysis*, 2004, **16**, 140.
17 K. R. Kneton and R. L. McCreery, *Anal. Chem.*, 1992, **64**, 2518.
18 H. Chang and A. J. Bard, *Langmuir*, 1991, **7**, 1143.
19 T. J. Davies, R. R. Moore, C. E. Banks and R. G. Compton, *J. Electroanal. Chem.*, 2004, **574**, 123.
20 J. C. Eklund, A. M. Bond, J. A. Alden and R. G. Compton, *Adv. Phys. Org. Chem.*, 1999, **32**, 1.
21 C. Amatore, J.-M. Savéant and D. Tessier, *J. Electroanal. Chem.*, 1983, **147**, 39.
22 T. J. Davies, B. A. Brookes and R. G. Compton, *J. Electroanal. Chem.*, 2004, **566**, 193.
23 T. J. Davies, A. C. Garner, S. G. Davies and R. G. Compton, *J. Electroanal. Chem.*, 2004, **570**, 171.
24 M. Rudolph, D. P. Reddy and S. W. Feldberg, *Anal. Chem.*, 1994, **66**, 589A.
25 M. T. McDermott, K. Kneten and R. L. McCreery, *J. Phys. Chem.*, 1992, **96**, 3124.
26 R. J. Bowling, R. T. Packard and R. L. McCreery, *J. Am. Chem. Soc.*, 1989, **111**, 1217.
27 A. J. Bard and L. R. Faulkner, *Electrochemical Methods*, Wiley, New York, 2nd edn., 2001, ch. 6.
28 K. K. Cline, M. T. McDermott and R. L. McCreery, *J. Phys. Chem.*, 1994, **98**, 5314.
29 R. J. Rice and R. L. McCreery, *Anal. Chem.*, 1989, **61**, 1637.
30 H. C. Leventis, I. Streeter, G. G. Wildgoose, N. S. Lawrence, L. Jiang, T. G. J. Jones and R. G. Compton, *Talanta*, 2004, **63**, 1039.
31 G. G. Wildgoose, H. C. Leventis, I. Streeter, N. S. Lawrence, S. J. Wilkins, L. Jiang, T. G. J. Jones and R. G. Compton, *ChemPhysChem*, 2004, **5**, 669.
32 G. G. Wildgoose, S. J. Wilkins, G. R. Williams, R. R. France, D. L. Carnahan, L. Jiang, T. G. J. Jones and R. G. Compton, *ChemPhysChem*, submitted 2004.
33 C. G. R. Heald, G. G. Wildgoose, L. Jiang, T. G. J. Jones and R. G. Compton, *ChemPhysChem*, 2004, **5**, 1794.
34 A. J. Downard, *Electroanalysis*, 2000, **12**, 1085.
35 B. Barbier, J. Pinson, G. Desarmot and M. Sanchez, *J. Electrochem. Soc.*, 1990, **137**, 1757.
36 M. Delamar, R. Hitimi, J. Pinson and J.-M. Savéant, *J. Am. Chem. Soc.*, 1992, **114**, 5883.
37 M. Pandurangappa, N. S. Lawrence and R. G. Compton, *Analyst*, 2002, **127**, 1568.
38 M. Pandurangappa, N. S. Lawrence, L. Jiang, T. G. J. Jones and R. G. Compton, *Analyst*, 2003, **128**, 473.
39 G. G. Wildgoose, M. Pandurangappa, N. S. Lawrence, L. Jiang, T. G. J. Jones and R. G. Compton, *Talanta*, 2003, **60**, 887.
40 A. Leonhardt, M. Ritschel, K. Bartsch, A. Graff, C. Taschner and J. Fink, *J. Phys. IV: Proceedings*, 2001, **11**, 445.
41 Y. Y. Wang, G. Y. Tang, F. A. M. Koeck, B. Brown, J. M. Garguilo and R. J. Nemanich, *Diamond Relat. Mater.*, 2004, **13**, 1287.

42 V. Z. Mordkovich, M. Baxendale, R. P. H. Chang and S. Yoshimura, *Synth. Met.*, 1997, **86**, 2049.
43 A. Pelekourtsa, N. Missaelidis and D. Jannakoudakis, *Chim. Chron.*, 1997, **26**, 39.
44 M. Hojo, K. Nishikawa, Y. Akita and Y. Imai, *Bull. Chem. Soc. Jpn.*, 1986, **59**, 3815.
45 K. Ray, III and R. L. McCreery, *Anal. Chem.*, 1997, **69**, 4680.
46 P. Allongue, M. Delamar, B. Desbat, O. Fagebaume, R. Hitimi, J. Pinson and J.-M. Savéant, *J. Am. Chem. Soc.*, 1997, **119**, 201.
47 Y.-C. Liu and R. L. McCreery, *J. Am. Chem. Soc.*, 1995, **117**, 11254.
48 Y.-C. Liu and R. L. McCreery, *Anal. Chem.*, 1997, **69**, 2091.
49 C. E. Banks, R. R. Moore, T. J. Davis and R. G. Compton, *Chem. Commun.*, 2004, **16**, 1804.
50 R. R. Moore, C. E. Banks and R. G. Compton, *Analyst*, 2004, **129**, 755.
51 J. Wang, M. Musameh and Y. Lin, *J. Am. Chem. Soc.*, 2003, **125**, 2408.